Title

Euchromatin factors HULC and Set1C affect heterochromatin organization for mating-type switching in fission yeast *Schizosaccharomyces pombe*

Authors

Alfredo Esquivel Chavez [1, 2], Takahisa Maki[2, *, †], Hideo Tsubouchi[1, 2], Testuya Handa[2, ‡], Hiroshi Kimura[1, 2], James E. Haber[3], Genevieve Thon[4], Hiroshi Iwasaki[1, 2, *]

Affiliations

[1] Department of Life Science and Technology, School of Life Science and Technology, Tokyo Institute of Technology, Yokohama, Kanagawa 226-8503, Japan

[2] Institute of Innovative Research, Tokyo Institute of Technology, Yokohama, Kanagawa 226-8503, Japan

[3] Department of Biology and Rosenstiel Basic Medical Science Research Center, Brandeis University, Waltham, Massachusetts, 02154-9110, USA

[4] Department of Biology, University of Copenhagen, 2200, Copenhagen N, Denmark

† Current address: Department of Molecular Neuroscience, Faculty of Medical Science, University of Fukui, Fukui 910-1193, Japan

‡ Current address: Cancer Research UK Cambridge Institute, University of Cambridge, Li Ka Shing Centre, Cambridge, CB2 0RE, UK

*co-corresponding authors

E-mail: tmaki@u-fukui.ac.jp (TM), hiwasaki@bio.titech.ac.jp (HI)

Short title: Euchromatin factors HULC and Set1C regulate mating-type switching in *Schizosaccharomyces pombe*

Abstract

Mating-type switching (MTS) in fission yeast *Schizosaccharomyces pombe* is a highly regulated gene conversion event. In the process, heterochromatic donors of genetic information are selected based on the P or M cell type and on the use of two recombination enhancers, *SRE2* promoting use of *mat2-P* and *SRE3* promoting use of *mat3-M*. Recently, we found that the histone H3K4 methyltransferase complex Set1C participates in donor selection, raising the question of how a complex best known for its effects in euchromatin controls recombination in heterochromatin. Here, we report that the histone H2BK119 ubiquitin ligase complex HULC functions with Set1C in MTS, as mutants in the *shf1*, *brl1*, *brl2* and *rad6* genes showed defects similar to Set1C mutants and belonged to the same epistasis group as *set1*Δ. Moreover, using H3K4R and H2BK119R histone mutants and a Set1-Y897A catalytic mutant indicated that ubiquitylation of histone H2BK119 by HULC and methylation of histone H3K4 by Set1C are functionally coupled in MTS. Cell-type biases in mutants further showed that the regulation might be by inhibiting use of the *SRE3* enhancer in M cells, in favor of *SRE2*. Consistently, imbalanced switching in the mutants was traced to compromised association of the directionality factor Swi6 with the recombination enhancers in M cells. Based on their known effects at other chromosomal locations, we speculate that HULC and Set1C might control nucleosome mobility and strand invasion near the *SRE* elements. In addition, we uncovered distinct effects of HULC and Set1C on histone H3K9 methylation and gene silencing, consistent with additional functions in the heterochromatic domain.

Author Summary

Mating-type switching in the fission yeast *Schizosaccharomyces pombe* occurs by gene conversion using a donor, *mat2* or *mat3* located in a heterochromatin region. Multiple studies have shown that donor selection is critically affected by heterochromatic factors. Here, we document the role of euchromatic factors, the histone H2BK119 ubiquitin ligase complex HULC and the H3K4 methyltransferase complex Set1C, in donor selection. Mutational analysis indicated that HULC and Set1C inhibit donor choice at the *mat3 cis*-acting recombination enhancer *SRE3* in M cells, through concerted histone modifications by the two complexes. Linking this effect with heterochromatin, mutants in each complex, *shf1*Δ and *set1*Δ strains, exhibited decreased association of the HP1 heterochromatic factor Swi6 with the *SRE2* and *SRE3* recombination enhancers at the *mat2* and *mat3* silent loci in M cells. These joint effects by the two complexes on MTS were observed even though other aspects, the methylation state

of histone H3K9 and effects on gene silencing differed between the *shf1*Δ and *set1*Δ strains. The results provide insight into the regulation of recombination by chromatin structure.

Introduction

Homothallic strains (h^{90}) of the fission yeast *Schizosaccharomyces pombe* switch between two mating types, P and M. This process is known as mating-type switching (MTS) and it takes place at the *mat* locus on chromosome 2. The *mat* locus comprises three cassettes, *mat1*, *mat2* and *mat3* (Fig 1A). The active *mat1* cassette expresses either P or M mating-type specific genes and determines the mating-type of a haploid cell [1]. The genes in the *mat2* and *mat3* cassettes, P (*mat2-P*) and M (*mat3-M*), respectively, are invariant, and are silenced by heterochromatin. Each cassette is flanked by short homology boxes called *H1* and *H2*. MTS is a result of gene conversion of the *mat1* cassette by either the *mat2-P* or *mat3-M* donor cassette using the homology boxes [2].

A cell-type specific regulation takes place at the donor-selection step, where cells usually select the mating-type donor cassette opposite to the allele present at *mat1*, thus, P cells (*mat1-P*) preferentially choose *mat3-M* as a donor, while *mat1-M*, M cells (*mat1-M*) preferentially choose *mat2-P* (Fig 1B) [3]. This donor selection requires the mating-type switching factors Swi2 and Swi5, the heterochromatin protein 1 (HP1) homologue Swi6, and *cis*-acting DNA elements [4-6]. The *cis*-acting DNA elements are called Swi2-dependent Recombination Enhancers, *SRE2* and *SRE3*, and are located next to the *H1* box of *mat2-P* and *mat3-M*, respectively [4, 5]. The Swi2 protein localizes to these elements according to cell type: in P cells, Swi2 localizes only to *SRE3*; in M cells, Swi2 localizes to both *SRE2* and *SRE3* [4, 5]. From yeast two-hybrid assays, Swi2 has been shown to interact with Swi5 and with the recombination factor Rad51; therefore, it has been suggested that the Swi2-Swi5 complex promotes homologous recombination at the *SRE2*- or *SRE3*-adjacent cassette [7]. Furthermore, the Swi6 protein spreads at the *mat* locus between the boundary elements *IR-L* and *IR-R* and it contributes to form heterochromatin over the entire region [8, 9]. The association of Swi6 with the region differs between P and M cells, with greater enrichment of Swi6 in M cells than P cells [8]. As Swi2 interacts with Swi6 *in vitro*, the localization pattern of Swi2 is believed to be connected to its interaction with Swi6 [4, 7, 10].

Swi6 localization at the *mat* locus is controlled by several histone modifications [11]. An essential histone modification for Swi6 localization is di- or tri- methylation of histone H3 at lysine 9 (H3K9me2 and -me3, respectively) catalyzed by the methyltransferase Clr4, the homologue of human SUV39H1 and SUV39H2 [12-14]. H3K9me2 and -me3 are detected in constitutive heterochromatin such as *mat*, centromeres and telomeres, and in facultative heterochromatin such as meiotic genes [15, 16]. Constitutive heterochromatic regions contain repetitive DNA sequences that nucleate H3K9 methylation through RNA interference (RNAi)

[15]. At the *mat* locus, RNAi is triggered by the transcription of *cenH*, homologous to centromeric repeats [17, 18]. dsRNAs originating from *cenH* are cleaved by the ribonuclease Dcr1, and the siRNA products are bound by the RNAi-induced transcriptional silencing complex (RITS) [19, 20]. RITS loaded with siRNAs recruits the Clr4-Rik1-Cul4 complex (CLRC) to methylate H3K9 [21]. At the *mat* locus, there is an additional silencing pathway involving the CREB-like transcription factor, Atf1-Pcr1 [22]. The Atf1-Pcr1 dimer binds to consensus sequences within the *mat* locus that exist at the *REIII* silencer and ~1.4 k bp away from *REIII*, close to *cenH* (Fig 1A) [23]. Other histone-modifying enzymes such as histone deacetylases (HDACs) are also required for donor selection and heterochromatin establishment. These include the NAD^+-dependent histone deacetylase Sir2 [24] and the Snf/Hdac-containing repressor complex (SHREC), Clr1, Clr2 and Clr3 [12, 25]. Clr4, Clr3 and another HDAC, Clr6, interact with Atf1, therefore Atf1-Pcr1 has been suggested to recruit these histone modifying enzymes to the *mat* locus [22, 26, 27].

We recently conducted a genetic screen for factors that affect mating-type switching and we identified the six genes encoding the H3K4 mono-, di- and tri-methyltransferase complex, Set1C/COMPASS, as well as a component of the H2BK119 monoubiquitin ligase HULC [3, 28]. In *S. pombe*, no other enzyme catalyzes these reactions. Ubiquitylation of H2B (H2Bub at K119 in fission yeast, at K123 in budding yeast, and at K120 in human) is required for the tri-methylation of H3K4 by Set1/COMPASS family from yeast to human [29]. Therefore, we hypothesized that H2Bub and H3K4me might work together to regulate MTS. Interestingly, the histone modifications by HULC and Set1C are generally observed at active genes, in euchromatin, and have been proposed to antagonize heterochromatin formation at the *mat* locus [8, 30, 31]. However, HULC and Set1C have also been reported to have a positive effect on gene silencing in heterochromatin [32-34]. HULC was proposed to promote loading of heterochromatin factors in centromeric repeats by facilitating a wave of transcription that fuels the RNAi machinery during S-phase [32]. In the case of Set1C, the deletion of the catalytic subunit Set1 causes a slight derepression of centromeric and telomeric reporter genes, and transcription of the *cenH* element in the *mat* region [33, 34]. In addition, Set1C also functions in the repression of the stress-response gene *ste11* [35, 36] and *Tf2* retrotransposons [34]. Interestingly, Set1 localizes with Atf1 binding sites at centromeres, where it contributes to the heterochromatin assembly with the Clr3 HDAC [37].

In this study, we performed genetic and molecular analyses of HULC, Set1C, and histone mutants to better understand the role of the HULC and Set1C complexes in mating-type switching. Our results support the view that, like Set1C [38], HULC affects donor choice by

reducing the effectiveness of the *SRE3* enhancer in M cells and that H2B ubiquitylation by HULC and H3K4 methylation by Set1C operates in the same pathway for this function. Both modifying enzymes regulate Swi6 enrichment positively at the *SRE2* and *SRE3* elements. On the other hand, the two enzymes differentially affect heterochromatin formation and heterochromatic silencing at the *mat* locus. When combined with *dcr1*Δ, the *set1*Δ mutation caused a derepression of a reporter gene at *SRE3* while *shf1*Δ did not. Thus, beyond increasing our understanding of donor selection through HULC and Set1C, our findings also shed light on gene silencing mechanisms by these complexes.

Results

The histone H2B ubiquitylation complex HULC is involved in MTS

Recently, we determined that a subunit of HULC, the *brl2*$^{+}$ gene product, is required for efficient MTS by screening the gene deletion library, Bioneer version 5 [38]. In an independent screen for MTS defects with version 2 of the same library, we identified another subunit of HULC, the *shf1*$^{+}$ gene product. Therefore, we systematically investigated the switching phenotypes of mutants in each of the HULC subunits, the *shf1*Δ, *rad6*Δ, *brl1*Δ and *brl2*Δ mutants. MTS defects can be detected by measuring mating-type ratios in saturated liquid cell cultures because efficient switching results in an equal proportion of each cell type. Mutants in a few factors such as Swi2 mutants display different mating-type ratios in independent cultures while other mutations uniformly bias cell populations towards P or M [5, 38]. Thus, for each HULC mutant, four independent strains were analyzed to evaluate clonal variation by multiplex PCR. The wild-type *h*^{90} strain, PG4045, had nearly equal proportions of P and M cells, as expected, but all HULC mutants displayed a biased mating-type ratio which was around 33% P cells in all cultures examined (Figs 2A and S1A). The deletion mutants were also examined by iodine staining of colonies, a classical assay for MTS efficiency. Colonies of the control PG4045 strain grown on EMM plate stained darkly with iodine, indicative of efficient MTS, conjugation and sporulation during colony growth. The HULC mutants were less stained (Figs 2B and S1B) consistent with the observed cell-type bias. Double deletion of *shf1* and, respectively, *rad6*, *brl1* or *brl2* did not show any additive effect (Figs 2C and S1C). We concluded that HULC is involved in MTS.

The Rad18/Rad6 pathway does not influence MTS

In addition to its interaction with the E3 ubiquitin ligase Brl, the E2 Rad6 enzyme also operates with the E3 Rad18 in a conserved DNA damage tolerance pathway by mono-ubiquitylating PCNA [39]. We tested whether the Rad6/Rad18 pathway is required for MTS. As expected, both the *rad6* and *rad18* deletion mutant strains were sensitive to UV exposure, similar to a *rad51* deletion mutant strain (Fig 2D). On the other hand, HULC mutants, respectively *shf1*Δ, *brl1*Δ and *brl2*Δ, did not show UV damage sensitivity (Fig 2D). Conversely, multiplex PCR and iodine staining assays did not detect any switching defect in the *rad18*Δ mutant, unlike for the *shf1*Δ, *brl1*Δ and *brl2*Δ mutants (Figs 2A, B, S1A and S1B). These results indicate that Rad6 functions in different complexes for MTS and DNA damage tolerance.

HULC regulates donor selection at *SRE3*

Depending on which step is affected, mutants deficient in MTS can be separated into three classes, Class Ia, Class Ib and Class II, by Southern blots [6]. Class Ia mutants lack an imprint at *mat1*; the imprint is required for MTS as it is converted to a single-ended double-strand break just past the *H1* homology box during DNA replication, allowing invasion of *mat2-P* or *mat3-M* by the *H1* sequence (Fig 1) [2, 3]. The imprint also creates a fragile site that causes breakage during DNA preparation and it is thus visible on Southern blots as a DNA double-strand break. Class Ib mutants have the imprint but fail to use it properly. Class II mutants are deficient at a later step, in the resolution of the gene conversion, which causes characteristic *mat2-mat3* cassette duplications inserted at *mat1* that are not found in Class I mutants. The *shf1* deletion was assigned to Class Ib in which a functional imprint is detected at the *mat1* cassette (S2A Fig) similar to the previously examined *brl2* deletion [38]. The Class Ib group includes mutations that impair donor selection. These can be identified and further classified according to their effects in h^{09} cells that have swapped *mat2-M mat3-P* donor cassettes [40]. At least four groups of h^{09} Class Ib mutants can be distinguished: Group 1a displaying a strong bias towards P cells; Group 1b with a mild bias towards P cell; Group 2 with clonal variations; and Group 3 with a bias towards M cells [38]. Deletions removing HULC subunits each caused a mild bias towards P cells in the h^{09} background (~48 % P cells instead of ~19 % in the presence of functional HULC), placing them in Group 1b (Figs 3A and S2B).

The *SRE* elements are necessary for donor selection [4, 5]. We investigated the importance of *SRE2* and *SRE3* in the presence or absence of the *shf1* gene using *SRE* deletion mutants (Fig 3B). In an *SRE3*Δ strain, the *shf1* deletion did not affect the mating-type ratio (~ 83% P cells in *shf1*Δ instead of ~84 % in $shf1^+$ cells) (Figs 3B and S2C). In an *SRE2*Δ strain, the *shf1* deletion slightly affected the mating-type ratio towards M cells (~ 12% P cells in *shf1*Δ instead of ~19 % in $shf1^+$ cells) (Figs 3B and S2C). Taken together with the biases caused by HULC mutations in h^{90} (towards M cells, using *SRE3*) and h^{09} strains (towards P cells, using *SRE3*), these results suggest that, in M cells, HULC normally prevents the use of *SRE3*, rather than facilitating the use of *SRE2*.

Histone residues modified by HULC and Set1C are required for MTS

We noticed that the genetic analyses in Fig 3 showed similar trends for the MTS defects detected in HULC mutants and the defects previously reported for *set1* deletion mutants [38]. The ubiquitylation of H2BK119 by HULC is essential for H3K4me3 by Set1C in *S. pombe* [41], therefore we performed an epistasis analysis to test the relationship between HULC and Set1C in MTS. The switching defect of the h^{90} *shf1*Δ *set1*Δ double mutant was quite similar to the

switching defect of the h^{90} *set1*Δ strain (~42% P cells in *shf1*Δ *set1*Δ mutant *versus* ~43% P cells in *set1*Δ mutant in the multiplex PCR assay), with *set1*Δ slightly suppressing the cell-type bias of the *shf1*Δ strain (~33% P cells in *shf1*Δ mutant) (Figs 4A and S3A). This placed the two mutations in the same epistasis group, suggesting coordinated action of HULC and Set1C.

Next, we investigated the importance of the histone H2BK119 and H3K4 residues that are modified by HULC and Set1C, respectively, in MTS. The proportion of P cells in the H2BK119R mutant (~34% P cells) was not only similar to the *shf1*Δ deletion mutant, but also to the double mutant *shf1*Δ H2BK119R (Figs 4B and S3B). On the other hand, the proportion of P cells in the H3K4R mutant was ~27% P cells, less than in the *set1*Δ deletion mutant (~44% P cells), but similar to the H3K4R *set1*Δ double mutant (~30% P cells) (Figs 4B and S3C). We also investigated the requirement for the catalytic activity of Set1 in MTS. The SET domain has a highly conserved tyrosine residue which is suggested to be a catalytic residue from the crystal structure (S3D Fig) [42]. Replacement of tyrosine Y1054 with alanine in *S. cerevisiae* Set1 causes loss of H3K4 methylation [43]. We created a Set1-Y897A mutant in *S. pombe*, corresponding to Set1-Y1054A in *S. cerevisia*e (S3D Fig). The mating-type ratios in the *set1-Y897A* mutant analyzed by multiplex PCR were similar to the ratios in the *set1*Δ mutant (Figs 4D and S3E). We verified that the Set1-Y897A protein tagged with 9×V5 epitope (9×V5-Set1-Y897A) was present in the cells (S3F Fig). The $swd1^{+}$ gene encodes a subunit of the Set1C complex [41]. An *swd1*Δ single mutant and *swd1*Δ Set1-Y897A double mutant also showed similar ratios to the *set1*Δ mutant (Figs 4D and S3E). These observations point to both H2BK119 ubiquitylation by HULC and H3K4 methylation by Set1C playing an important role in the directionality of MTS.

Several lines of evidence have indicated that the RNA polymerase II-associated factor 1 complex Paf1C [44-46], functionally conserved from yeast to mammals [47, 48], can recruit HULC and Set1C [49] and in fission yeast Paf1C prevents heterochromatin propagation across the *IR-L* boundary of the *mat* locus, among other effects [49]. We constructed strains lacking the Paf1C components Leo1 and Paf1, respectively, to test the requirement for Paf1C in MTS. The *leo1*Δ and *paf1*Δ mutants did not show a switching defect in the multiplex PCR assay (Figs 4E and S3G). Thus, the effects of HULC and Set1C in MTS occur independently of Paf1C.

Set1 and Shf1 are involved in the mating-type-specific localization of Swi6 at *SRE2* and *SRE3*, but they have different effects on histone H3K9 methylation

The results presented so far allow updating a previous model [38] by now proposing that both HULC and Set1C reduce use of the *SRE3* recombination enhancer in M cells by modifying histone H2BK119 and H3K4. Given that differential Swi6 enrichment in the mating-type regions of M and P cells is a determinant of donor choice [4, 5, 40], we next investigated the effects of HULC and Set1C on Swi6 occupancy. To this end, we performed ChIP-qPCR with Flag-tag antibody for 3×Flag-Swi6 using heterothallic strains with a fixed mating type, P or M (Fig 5A). In a wild-type background, Swi6 showed an approximately three-fold higher enrichment at both *SRE2* and *SRE3* in M cells compared to P cells (Fig 5B). No significant difference between P and M cells was observed at the K region, a location between *mat2-P* and *cenH* (Fig 5B). In both the *shf1*Δ and *set1*Δ backgrounds, the high, M-specific, Swi6 occupancy at *SRE2* and *SRE3* was decreased (Fig 5B). It thus appears likely that Shf1 and Set1, and by extension HULC and Set1C, control donor choice at least in part by ensuring high Swi6 occupancy at recombination enhancers in M cells. We note however that the double *shf1*Δ *swi6*Δ deletion mutant showed a statistically significant slightly lower (in h^{90}) or higher (in h^{09}) proportion of P cells compared with the single *swi6*Δ mutant (S4 Fig), suggesting some effects of HULC in MTS are not through Swi6.

Swi6 recognizes di- and trimethylation of histone H3K9 [14, 50] . We thus examined the di- and tri- methylation levels of H3K9 in *shf1*Δ and *set1*Δ strains using the same chromatin fixed samples as in Fig 5B and antibodies specific for di- and tri- methylation of H3K9 (H3K9me2 and H3K9me3, respectively) (Fig 5C and D). Comparing P and M cells, we observed that H3K9me2 enrichments in wild-type strains were similar at the three locations examined and did not vary with cell type, with the possible exception of *SRE2* for which H3K9me2 was slightly lower in M cells (Fig 5C). In *shf1*Δ strains, H3K9me2 was significantly reduced in both cell types with the similar tendency of slightly lower enrichments in M cells (Fig 5C). The opposite trend was seen for *set1*Δ cells where H3K9me2 was unchanged or, in the case of M cells, increased (Fig 5C).

For H3K9me3, M cells showed somewhat higher enrichments than P cells in the wild-type background (Fig 5D). This difference between P and M cells was attenuated in the *shf1*Δ background, but globally the levels of H3K9me3 enrichments remained unchanged in *shf1*Δ cells (Fig 5D). As observed for H3K9me2 (Fig 5C), H3K9me3 levels were increased by *set1*Δ, at all locations and in both cell types (Fig 5D). These ChIP-qPCR analyses suggest that the enrichment levels of H3K9me2 and H3K9me3 are regulated by Shf1 and Set1, however these regulations work in different manners and correlations between H3K9 methylation and Swi6 enrichment levels were not systematically observed.

Shf1 and Set1 have differential effects on silencing and MTS

Two main pathways of heterochromatin formation have been well documented at the *mat* locus, one is RNAi nucleating heterochromatin at the *cenH* region [15, 17, 18], and the other is an RNAi-independent pathway involving the Atf1-Pcr1 complex [22, 26, 51, 52]. Both H2Bub and H3K4me are believed to control transcription by regulating RNA polymerase II activity in *S. pombe* [31, 34, 53]. This suggests that HULC and Set1C might participate in silencing the *mat* locus by facilitating RNAi which uses transcription products from *cenH* to nucleate heterochromatin. Alternatively, the fact that H2Bub and H3K4me mediate gene silencing at the *ste11* gene locus [35, 36], together with the fact that Set1 localizes to Atf1 binding sites at centromeres and at the *ste11* gene locus [37], suggests that HULC and Set1C might co-operate with Atf1-Pcr1 also in the mating-type region. To investigate whether Shf1 or Set1 participate in the RNAi or Atf1-Pcr1 pathway of heterochromatin formation, we created double mutants, respectively *shf1*Δ *dcr1*Δ, *shf1*Δ *pcr1*Δ, *set1*Δ *dcr1*Δ and *set1*Δ *pcr1*Δ in a strain with a *ura4*$^{+}$ reporter gene inserted in the *SRE3* region (PG1899 with *(EcoRV)::ura4*$^{+}$) (Fig 6A). As previously reported [22], *dcr1*Δ and *pcr1*Δ single deletion mutants with the *(EcoRV)::ura4*$^{+}$ reporter were resistant to 5-FOA, which is toxic to cells that express *ura4*$^{+}$, while the *dcr1*Δ *pcr1*Δ double deletion caused sensitivity, which was the same level as the *swi6*Δ strain (Fig 6B). The *shf1*Δ single mutant was resistant to 5-FOA, and the *shf1*Δ *dcr1*Δ and *shf1*Δ *pcr1*Δ double mutants remained resistant. In contrast, the *set1*Δ and *set1*Δ *pcr1*Δ strains were resistant to 5-FOA, but the *set1*Δ *dcr1*Δ strain was clearly sensitive, its growth on 5-FOA was as severely affected as growth of the *dcr1*Δ *pcr1*Δ strain (Fig 6B). This places *set1*Δ, but not *shf1*Δ, in the same epistasis group as *pcr1*Δ for the effects of these mutations on silencing in the mating-type region.

We examined the switching phenotype of the strains shown in Fig 6B by multiplex PCR (Figs 6C and S5). The PG1899 strain was slightly biased toward P cells (~59% P cells) in comparison with the normal h^{90} configuration (~50% P cells). This switching phenotype probably comes from the insertion of the *ura4*$^{+}$ gene slightly affecting *SRE3* due to its proximity (see Fig 6A). However, populations of a *swi6*Δ derivative of PG1899 showed mating-type biases similar to the h^{90} *swi6*Δ mutant, hence we analyzed all mutant strains derived from PG1899 for MTS. The single *dcr1*Δ and *pcr1*Δ mutants showed mating-type ratios similar to PG1899. The double *dcr1*Δ *pcr1*Δ mutant was biased towards M cells (~45% P cells). The double *shf1*Δ *dcr1*Δ and *shf1*Δ *pcr1*Δ mutants had cell-type ratios similar to the *shf1*Δ single deletion mutant. In the case of *set1*Δ, the *set1*Δ *pcr1*Δ deletion strain had a cell-type ratio

similar to the *set1*Δ strain, but the *set1*Δ *dcr1*Δ double deletion strain showed a larger bias toward M cells than the *set1*Δ strain, the largest bias of all strains examined. Thus, both gene silencing and multiplex PCR assays converge to show that Set1 functions in parallel to Dcr1 at the silent *mat* locus.

Discussion

Mating-type switching is governed by chromatin conformation. Thus, the H3K9 methyltransferase CLRC and several HDACs have well documented roles on the formation of heterochromatin required for the directionality of switching. Our genetic screens identified euchromatic factors, the H2B ubiquitin ligase HULC and the H3K4 methyltransferase Set1C, as additional MTS factors (Fig 2) [38]. A potentially important feature is that these complexes engage in a cross-talk where H2B ubiquitylation upregulates H3K4 methylation by Set1C [53]. Here, we obtained evidence that HULC and Set1C function in a common pathway for MTS to inhibit the preferential use of the *SRE3* enhancer in M cells, plausibly through this crosstalk. Notably, the effects of the two complexes determined by mutational analyses were not quite identical and distinct contributions to gene silencing were detected for Set1 and Shf1 that are likely to reflect some divergent functions in heterochromatin formation.

Strong biases towards the M cell-type were observed in both HULC and Set1C mutants denoting increased use of the *SRE3* enhancer in these mutants (Figs 2 and 3) [28]. An epistasis analysis assigned the two complexes to the same pathway (Fig 4), even though a slightly more pronounced bias towards M cells was observed in *shf1*Δ cells than in *set1*Δ or *shf1*Δ *set1*Δ cells (Fig 4A). It has been reported that Set1 is still expressed in cells that lack HULC and ubiquitylation of H2BK119 *in vivo* [31, 34, 53] and H3K4 di-methylation is slightly detected in H2BK119R strain [53]. In *S. cerevisiae*, H3K4 mono-methylation is still detected in *rad6* deletion cells [54]. Therefore, we speculate that the residual mono- and/or di- methylation of H3K4 in cells lacking H2Bub might increase the bias towards M cells, either directly through effects on recombination or indirectly. Our study also revealed that while the H2BK119R, *shf1*Δ and combined H2BK119R *shf1*Δ mutations had the same effect on MTS (Fig 4B), the switching defects in the H3K4R and H3K4R *set1*Δ mutants were much stronger than in the single *set1*Δ strain (Fig 4C). Transient acetylation of H3K4 has been proposed to facilitate the association of Swi6 with histone H3K9me2 through a chromodomain switch where Swi6 replaces H3K9me2-bound Chp1 or Clr4 at centromeres [55]. The same mechanism facilitating Swi6 association at *SRE* elements at the *mat* locus might account for the pronounced effects of H3K4R on MTS where Swi6 association is paramount.

The differential association of Swi6 with the mating-type region is a distinguishing factor between P and M cells: Swi6 is present at a low level over the region in P cells, coinciding with Swi2 specifically at *SRE3*, but at a high level in M cells, coinciding with Swi2 at both *SRE2* and *SRE3* [4]. These associations are believed to favor the use of *SRE2* over *SRE3* in M cells [5, 56]. We found here that Shf1 (and to a lesser extent Set1) is required for the high

Swi6 occupancy at *SRE2* and *SRE3* in M cells. In the *shf1*Δ and *set1*Δ mutants, Swi6 occupancy remained abnormally low at both enhancers in M cells, similar to what is normally seen in P cells (Fig 5). This profile could account for *SRE3* being preferred over *SRE2* in both cell types in the mutants, where all cells would in essence behave as P cells. The association of Swi6 with the enhancers was most strongly reduced in the *shf1*Δ mutant (Fig 5), where donor choice was also most impaired (Fig 4). These effects would place HULC and Set1C upstream of the enhanced Swi6 association with recombination enhancers in M cells (Fig 6D), without excluding other points of action.

Our experiments are consistent with and support an active repression by HULC and Set1C at *SRE3*, relevant to the central question of how *SRE2* outcompetes *SRE3* in M cells when Swi2 is present at both enhancers. *SRE2* might be inherently more efficient than *SRE3* under the conditions, or recombination might be actively repressed at *SRE3*. Here, *shf1*Δ and *set1*Δ mutants showed a bias towards M cells in h^{90} cells (Figs 2 and 4) and towards P cells in h^{09} cells (Fig 3A), consistent with the two factors repressing use of *SRE3*. Moreover, the ~80% bias towards P in *SRE3*Δ cells remained unchanged in the *shf1*Δ mutant, indicating *SRE2* is functional in the absence of Shf1. In contrast, in the *SRE2*Δ strain, *SRE3* was increasingly used in *shf1*Δ cells, indicating Shf1 inhibits use of *SRE3* (Fig 3B). Thus, our genetic analyses suggest that HULC inhibits selection of *SRE3* - and thereby *mat3-M* donor selection - in h^{90} cells, similar to Set1C (Fig 6D) [28].

How might an inhibition of recombination by HULC/Set1C take place at *SRE3*? A relevant effect of HULC/Set1C could be by controlling nucleosome occupancy or positioning. In *S. cerevisiae*, nucleosome occupancy is decreased genome-wide in H2BK123, *rad6*Δ, and *lge1*Δ mutants [57, 58]. In *S. pombe*, H2Bub decreases chromatin remodeling by RSC at the *ste11* promoter to repress transcription [35, 36]. In this case, the effect of H2Bub is through H3K4me and histone deacetylation, supporting the idea that HULC, Set1C, and HDACs might work in concert to position nucleosomes at the *mat* locus as well. Nucleosome positioning at *SRE3* might mask the enhancer or prevent strand invasion. An intriguing alternative that our results do not exclude is that nucleosome positioning or modification by HULC/Set1C might facilitate recombination near *SRE2* in M cells. Positive effects on recombination repair and on recombination-dependent bypass of DNA lesions have been reported for the RNF20/RNF40 mammalian homolog of Bre1 [59, 60] and for the *S. cerevisiae* counterpart of HULC [61]. Nucleosome depletion by associated remodelers, rather than nucleosome stabilization, often appears instrumental during repair, highlighting the context dependency of the effects of the modifying and remodeling complexes [60, 62]. It will be important in the future to understand

how remodeling complexes might contribute to MTS, taking into account the fact that Swi6 also interacts with many remodelers [63].

Finally, we uncovered effects of HULC and Set1C on the heterochromatic structure of the mating-type region that bring light to how these complexes might affect Swi6 association and MTS. In the case of *shf1*Δ, we observed reduced H3K9me2 at the three locations tested (Fig 5C). HULC has been suggested to associate with the RNAi machinery in centromeric region when repetitive sequences are transcribed during S-phase [32], by analogy *cenH* in the mating-type region might be an entry point for HULC. In the case of *set1*Δ, we observed a synthetic silencing defect when combining the *set1*Δ and *dcr1*Δ mutations (Fig. 6B), showing that Set1 and Dcr1 participate in parallel pathways of heterochromatin formation. The effect is clearly relevant to MTS as the double mutant showed a strong bias towards M cells (Fig 6C). Similarly, Dcr1 and the Clr3 HDAC operate in parallel to recruit Clr4 to the *mat* locus, Dcr1 through RNAi at *cenH* and Clr3 through the Atf1-Pcr1 binding sites [27]. Here, we placed *set1*Δ in the same epistasis group as *pcr1*Δ for the effects of these mutations on silencing (Fig 6B), suggesting that the Atf1-Pcr1 binding sites at the *mat* locus constitute entry points not just for Clr3 but also for Set1C. Independently, a genome-wide study found that Set1 cooperates with Clr3 to repress transcription at other Atf1-Pcr1 binding sites [37] and an important effect of Clr3 in heterochromatin is to suppress histone turnover [51, 52, 64]. Thus, taken altogether, HULC and Set1C might be recruited in several ways to the *mat* locus where they would cooperate with Clr3 to regulate aspects of heterochromatin formation and nucleosome occupancy important for donor selection. To further analyze this mechanism, we will need to understand how the regulation would be exerted in a cell-type-specific manner, as well as spatially, whether the regulation has to occur locally at the enhancers, or whether global effects on nucleosome mobility that would differ in P and M cells might lead to the observed biases in enhancer use.

Material and Methods

Yeast strains, strains constructions and strain manipulations

S. pombe strains used in this study are described in S1 Table. Standard techniques were used to cultivate, sporulate, cross and genetically manipulate *S. pombe* [65]. Strains were generated by transformations or genetic crosses. The H3K4R mutant strain (TM504: h^{90} *hht1-H3K4R hht2-H3K4R leu1-32 his3-D1*) was generated from EM20 (h^{90} *leu1-32 his3-D1 ade6-M375*) by CRISPR/Cas9-mediated gene editing. EM20 was transformed by a gRNA expression plasmid (pEM59), a Cas9 expression plasmid and HR donor templates. To mutate the *hht1 and hht2* genes, the common target sequence, 5'-TCTACCGGTGGTAAGGCACC-3', was inserted into the gRNA scaffold portion in pEM59. To select cells in which Cas9 was active, the *ade6-M375* mutation was edited in the same transformation. The gRNA targeting *ade6-M375*, 5' CCTGCCAAACAAATTGATTG was also expressed from pEM59. The HR donor templates for mutagenesis, purchased from Integrated DNA Technologies, were amplified using primer sets, *hht1-H3K4R:* (5'-CTGCAGTACGCTTGCGTTTC-3' and 5'-GGGACGATAACGATGAGGCTTC-3'), *hht2-H3K4R* (5'-GGGAAGCCGAAATCGCAATC-3' and 5'-CCAGGACGATAACGATGAGGCTTC-3') and $ade6^{+}$ (5'-GTGGTCAATTGGGCCGTAT-3' and 5'-CGTGCACTTCTTAGACAGTTCA-3') by PCR. Cells were grown on low-adenine plates and white colonies ($ade6^{+}$) were selected. TM863 and TM896 were derived from TM504. TM501 was also generated by Cas9-mediated gene editing, with the gRNA target sequence (5'-TACTTATGATTACAAGTTTC-3') and the HR donor template amplified by primer set (5'-GGGAAATATCGCGCGTTTC-3' and 5'-CTAGTTTAAATAGCCACGACATGT-3'). All mutants selected for further analysis were confirmed by PCR and sequence analysis.

Iodine staining

Cells were streaked on MSA plates, grown at 26°C for 3~4 days and colonies were exposed to iodine vapors.

Multiplex PCR

Isolated colonies of the strains of interest were propagated in 2 ml YE5S cultures at 30°C, to saturation. 500 µl of each culture were harvested in a 1.5 ml microcentrifuge tube, followed by DNA extraction with a Dr. GenTLE (from yeast) high recovery kit (Takara Bio). Quantification of genomic DNA concentration was performed using the Quantifluor® ONE dsDNA Dye System (Promega). Multiplex PCR was performed as previously described [28].

UV damage sensitivity

Serial dilutions of exponentially growing cell cultures were plated on complete medium (YES) and subjected to UV irradiation by exposure to a germicidal lamp (254 nm; 100 J/m^2). UV intensities were measured with a UV Radiometer (TOPCON UVR-2). Plates were incubated at 30°C for 3~4 days.

Chromatin Immunoprecipitation (ChIP)

ChIP was performed as in Kimura et al., 2008 with a few modifications [66]. EMM2 medium (50 mL) containing 0.1 g/l each of leucine, adenine, histidine, uracil and arginine was used for cell culture. The cultures were propagated to 1.0×10^7 cells/ml at 30°C, and then shifted to 18°C for 2 h. 5.0×10^8 cells were cross-linked with 1% formaldehyde for 15 min at 25°C and then incubated in 125 mM glycine for 5 min. Cross-linked cell lysates were solubilized by a multi-beads shocker (Yasui Kikai) at 4°C, 15 cycle of 1 min on and 1 min off, and sonicated using a Bioruptor UCD-200 (Diagenode) at 2 cycle of 10 min each with alternating pulses of 40 sec on and 30 sec off at high level. The sheared samples were centrifuged at 20,000 g for 10 min at 4°C. The supernatants were incubated with 30 μl Dynabeads Protein A (Thermo Fisher) preloaded with 1.2 μl anti-FLAG M2 antibody (Sigma-Aldrich) for 6 h at 4°C. The beads were washed sequentially with wash buffer 1 (50 mM Hepes-KOH [pH7.5], 1 mM EDTA, 0.1 % Sodium deoxycholate, 0.5 M NaCl), wash buffer 2 (10 mM Tris-HCl [pH8.0], 0.25 M LiCl, 1 mM EDTA, 0.5% NP40, 0.5% SDS) and TE (twice), and materials coprecipitated with the beads were eluted with elution buffer (50 mM Tris-HCl [pH 7.6], 10 mM EDTA and 1% SDS) for 20 min at 65°C. The eluates were incubated at 65°C overnight to reverse cross-links and were then treated with 10 μg/ml RNase A for 1 hr at 37°C, followed by 20 μg/ml proteinase K for 3 hr at 50°C. DNA was purified with a MonoFas DNA purification kit I (GL Sciences). Quantitative PCR was performed with SYBR Premix Ex Taq II (TaKaRa Bio) or TB Green Premix DimerEraser (Takara Bio) on a Mx3000P qPCR system (Agilent). Primer sequences are in S2 Table B. For ChIP of H3K9me2 and -me3, 20 μg of H3K9me2 antibody or 20 μg of H3K9me3 antibody [67] were preloaded to 40 μl Dynabeads M-280 Sheep anti-Mouse IgG (Thermo Fisher).

Acknowledgments

We are grateful to members of the Iwasaki Laboratory for discussion. We thank to Jason Tanny for providing us with the *htb1* mutant strain and Jun-ichi Nakayama for providing us with the Flag-Swi6 strain. We thank the Biomaterials Analysis Division, Open Facility Center, Tokyo Institute of Technology for sequence analysis.

Funding

We acknowledge the following grant support: Grants-in-Aid for Scientific Research (A) (JP18H03985) to HI, for Scientific Research (B) (JP18H02371) to HT, and for Scientific Research on Innovative Areas (JP18H05527) to HK from the Japan Society for the Promotion of Science (JSPS); grant R35 GM127029 to JEH from NIH; the World Research Hub Initiative (WHRI) program at the Tokyo Institute of Technology to JEH; grant R167-A11089 to GT from the Danish Cancer Research Society; Otsuka Toshimi Scholarship Foundation to AEC.

Author contributions

A.E.C. and T.M. conducted experiments. T.M. and H.I. were responsible for conceptualization and project design. T.M., H.T., T.H., H.K., G.T. and H.I. supervised the study. H.K. provided materials. A.E.C., T.M., J.E.H, G.T and H.I. wrote the manuscript. T.M., J.E.H, G.T and H.I. were responsible for data analysis and funding acquisition.

Conflict of interest

The authors have no conflicts of interest to declare.

References

1. Kelly M, Burke J, Smith M, Klar A, Beach D. Four mating-type genes control sexual differentiation in the fission yeast. EMBO J. 1988;7(5):1537-47. PubMed PMID: 2900761; PubMed Central PMCID: PMCPMC458406.
2. Klar AJS, Ishikawa K, Moore S. A Unique DNA Recombination Mechanism of the Mating/Cell-type Switching of Fission Yeasts: a Review. Microbiol Spectr. 2014;2(5). Epub 2015/06/25. doi: 10.1128/microbiolspec.MDNA3-0003-2014. PubMed PMID: 26104357.
3. Thon G, Maki T, Haber JE, Iwasaki H. Mating-type switching by homology-directed recombinational repair: a matter of choice. Curr Genet. 2019;65(2):351-62. Epub 2018/11/02. doi: 10.1007/s00294-018-0900-2. PubMed PMID: 30382337; PubMed Central PMCID: PMCPMC6420890.
4. Jia S, Yamada T, Grewal SI. Heterochromatin regulates cell type-specific long-range chromatin interactions essential for directed recombination. Cell. 2004;119(4):469-80. doi: 10.1016/j.cell.2004.10.020. PubMed PMID: 15537537.
5. Jakociunas T, Holm LR, Verhein-Hansen J, Trusina A, Thon G. Two portable recombination enhancers direct donor choice in fission yeast heterochromatin. PLoS Genet. 2013;9(10):e1003762. doi: 10.1371/journal.pgen.1003762. PubMed PMID: 24204285; PubMed Central PMCID: PMCPMC3812072.
6. Egel R, Beach DH, Klar AJ. Genes required for initiation and resolution steps of mating-type switching in fission yeast. Proc Natl Acad Sci U S A. 1984;81(11):3481-5. PubMed PMID: 6587363; PubMed Central PMCID: PMCPMC345532.
7. Akamatsu Y, Dziadkowiec D, Ikeguchi M, Shinagawa H, Iwasaki H. Two different Swi5-containing protein complexes are involved in mating-type switching and recombination repair in fission yeast. Proc Natl Acad Sci U S A. 2003;100(26):15770-5. doi: 10.1073/pnas.2632890100. PubMed PMID: 14663140; PubMed Central PMCID: PMCPMC307643.
8. Noma K, Allis CD, Grewal SIS. Transitions in distinct histone H3 methylation patterns at the heterochromatin domain boundaries. Science. 2001;293(5532):1150-5. doi: DOI 10.1126/science.1064150. PubMed PMID: WOS:000170432600064.
9. Thon G, Bjerling P, Bunner CM, Verhein-Hansen J. Expression-state boundaries in the mating-type region of fission yeast. Genetics. 2002;161(2):611-22. PubMed PMID: 12072458; PubMed Central PMCID: PMCPMC1462127.
10. Akamatsu Y, Tsutsui Y, Morishita T, Siddique MS, Kurokawa Y, Ikeguchi M, et al. Fission yeast Swi5/Sfr1 and Rhp55/Rhp57 differentially regulate Rhp51-dependent recombination outcomes. EMBO J. 2007;26(5):1352-62. doi: 10.1038/sj.emboj.7601582. PubMed PMID: 17304215; PubMed Central PMCID: PMCPMC1817630.
11. Allshire RC, Madhani HD. Ten principles of heterochromatin formation and function. Nat Rev Mol Cell Biol. 2018;19(4):229-44. Epub 2017/12/14. doi: 10.1038/nrm.2017.119. PubMed PMID: 29235574; PubMed Central PMCID: PMCPMC6822695.
12. Ekwall K, Ruusala T. Mutations in rik1, clr2, clr3 and clr4 genes asymmetrically derepress the silent mating-type loci in fission yeast. Genetics. 1994;136(1):53-64. PubMed PMID: 8138176; PubMed Central PMCID: PMCPMC1205792.
13. Rea S, Eisenhaber F, O'Carroll D, Strahl BD, Sun ZW, Schmid M, et al. Regulation of chromatin structure by site-specific histone H3 methyltransferases. Nature. 2000;406(6796):593-9. Epub 2000/08/19. doi: 10.1038/35020506. PubMed PMID: 10949293.
14. Nakayama J, Rice JC, Strahl BD, Allis CD, Grewal SI. Role of histone H3 lysine 9 methylation in epigenetic control of heterochromatin assembly. Science. 2001;292(5514):110-3. doi: 10.1126/science.1060118. PubMed PMID: 11283354.

15. Allshire RC, Ekwall K. Epigenetic Regulation of Chromatin States in Schizosaccharomyces pombe. Cold Spring Harb Perspect Biol. 2015;7(7):a018770. Epub 2015/07/03. doi: 10.1101/cshperspect.a018770. PubMed PMID: 26134317; PubMed Central PMCID: PMCPMC4484966.
16. Zofall M, Yamanaka S, Reyes-Turcu FE, Zhang K, Rubin C, Grewal SI. RNA elimination machinery targeting meiotic mRNAs promotes facultative heterochromatin formation. Science. 2012;335(6064):96-100. Epub 2011/12/07. doi: 10.1126/science.1211651. PubMed PMID: 22144463; PubMed Central PMCID: PMCPMC6338074.
17. Hall IM, Shankaranarayana GD, Noma K, Ayoub N, Cohen A, Grewal SI. Establishment and maintenance of a heterochromatin domain. Science. 2002;297(5590):2232-7. doi: 10.1126/science.1076466. PubMed PMID: 12215653.
18. Volpe TA, Kidner C, Hall IM, Teng G, Grewal SI, Martienssen RA. Regulation of heterochromatic silencing and histone H3 lysine-9 methylation by RNAi. Science. 2002;297(5588):1833-7. Epub 2002/08/24. doi: 10.1126/science.1074973. PubMed PMID: 12193640.
19. Irvine DV, Zaratiegui M, Tolia NH, Goto DB, Chitwood DH, Vaughn MW, et al. Argonaute slicing is required for heterochromatic silencing and spreading. Science. 2006;313(5790):1134-7. Epub 2006/08/26. doi: 10.1126/science.1128813. PubMed PMID: 16931764.
20. Buker SM, Iida T, Buhler M, Villen J, Gygi SP, Nakayama J, et al. Two different Argonaute complexes are required for siRNA generation and heterochromatin assembly in fission yeast. Nat Struct Mol Biol. 2007;14(3):200-7. Epub 2007/02/21. doi: 10.1038/nsmb1211. PubMed PMID: 17310250.
21. Zhang K, Mosch K, Fischle W, Grewal SI. Roles of the Clr4 methyltransferase complex in nucleation, spreading and maintenance of heterochromatin. Nat Struct Mol Biol. 2008;15(4):381-8. doi: 10.1038/nsmb.1406. PubMed PMID: 18345014.
22. Jia S, Noma K, Grewal SI. RNAi-independent heterochromatin nucleation by the stress-activated ATF/CREB family proteins. Science. 2004;304(5679):1971-6. Epub 2004/06/26. doi: 10.1126/science.1099035. PubMed PMID: 15218150.
23. Thon G, Bjerling KP, Nielsen IS. Localization and properties of a silencing element near the mat3-M mating-type cassette of Schizosaccharomyces pombe. Genetics. 1999;151(3):945-63. PubMed PMID: 10049914; PubMed Central PMCID: PMCPMC1460531.
24. Shankaranarayana GD, Motamedi MR, Moazed D, Grewal SIS. Sir2 Regulates Histone H3 Lysine 9 Methylation and Heterochromatin Assembly in Fission Yeast. Current Biology. 2003;13(14):1240-6. doi: 10.1016/s0960-9822(03)00489-5.
25. Thon G, Klar AJ. The clr1 locus regulates the expression of the cryptic mating-type loci of fission yeast. Genetics. 1992;131(2):287-96. PubMed PMID: 1644273; PubMed Central PMCID: PMCPMC1205004.
26. Kim HS, Choi ES, Shin JA, Jang YK, Park SD. Regulation of Swi6/HP1-dependent heterochromatin assembly by cooperation of components of the mitogen-activated protein kinase pathway and a histone deacetylase Clr6. J Biol Chem. 2004;279(41):42850-9. doi: 10.1074/jbc.M407259200. PubMed PMID: 15292231.
27. Yamada T, Fischle W, Sugiyama T, Allis CD, Grewal SI. The nucleation and maintenance of heterochromatin by a histone deacetylase in fission yeast. Mol Cell. 2005;20(2):173-85. doi: 10.1016/j.molcel.2005.10.002. PubMed PMID: 16246721.
28. Maki T, Ogura N, Haber JE, Iwasaki H, Thon G. New insights into donor directionality of mating-type switching in Schizosaccharomyces pombe. Plos Genetics. 2018;14(5). doi: ARTN e1007424. doi: 10.1371/journal.pgen.1007424. PubMed PMID: WOS:000434016500047.

29. Shilatifard A. The COMPASS family of histone H3K4 methylases: mechanisms of regulation in development and disease pathogenesis. Annu Rev Biochem. 2012;81:65-95. Epub 2012/06/06. doi: 10.1146/annurev-biochem-051710-134100. PubMed PMID: 22663077; PubMed Central PMCID: PMCPMC4010150.
30. Greenstein RA, Barrales RR, Sanchez NA, Bisanz JE, Braun S, Al-Sady B. Set1/COMPASS repels heterochromatin invasion at euchromatic sites by disrupting Suv39/Clr4 activity and nucleosome stability. Genes & Development. 2020;34(1-2):99-117. doi: 10.1101/gad.328468.119. PubMed PMID: WOS:000505172100009.
31. Zofall M, Grewal SIS. HULC, a histone H2B ubiquitinating complex, modulates heterochromatin independent of histone methylation in fission yeast. Journal of Biological Chemistry. 2007;282(19):14065-72. doi: 10.1074/jbc.M700292200. PubMed PMID: WOS:000246245800016.
32. Chen ES, Zhang K, Nicolas E, Cam HP, Zofall M, Grewal SI. Cell cycle control of centromeric repeat transcription and heterochromatin assembly. Nature. 2008;451(7179):734-7. doi: 10.1038/nature06561. PubMed PMID: 18216783.
33. Kanoh J, Francesconi S, Collura A, Schramke V, Ishikawa F, Baldacci G, et al. The fission yeast spSet1p is a histone H3-K4 methyltransferase that functions in telomere maintenance and DNA repair in an ATM kinase Rad3-dependent pathway. Journal of Molecular Biology. 2003;326(4):1081-94. doi: 10.1016/S0022-2836(03)00030-5. PubMed PMID: WOS:000181401900010.
34. Mikheyeva IV, Grady PJ, Tamburini FB, Lorenz DR, Cam HP. Multifaceted genome control by Set1 Dependent and Independent of H3K4 methylation and the Set1C/COMPASS complex. PLoS Genet. 2014;10(10):e1004740. doi: 10.1371/journal.pgen.1004740. PubMed PMID: 25356590; PubMed Central PMCID: PMCPMC4214589.
35. Materne P, Anandhakumar J, Migeot V, Soriano I, Yague-Sanz C, Hidalgo E, et al. Promoter nucleosome dynamics regulated by signalling through the CTD code. Elife. 2015;4. doi: ARTN e09008
10.7554/eLife.09008. PubMed PMID: WOS:000374259100001.
36. Materne P, Vazquez E, Sanchez M, Yague-Sanz C, Anandhakumar J, Migeot V, et al. Histone H2B ubiquitylation represses gametogenesis by opposing RSC-dependent chromatin remodeling at the ste11 master regulator locus. Elife. 2016;5. doi: ARTN e13500. doi: 10.7554/eLife.13500. PubMed PMID: WOS:000376391000001.
37. Lorenz DR, Meyer LF, Grady PJ, Meyer MM, Cam HP. Heterochromatin assembly and transcriptome repression by Set1 in coordination with a class II histone deacetylase. Elife. 2014;3:e04506. doi: 10.7554/eLife.04506. PubMed PMID: 25497836; PubMed Central PMCID: PMCPMC4383021.
38. Maki T, Ogura N, Haber JE, Iwasaki H, Thon G. New insights into donor directionality of mating-type switching in Schizosaccharomyces pombe. PLoS Genet. 2018;14(5):e1007424. Epub 2018/06/01. doi: 10.1371/journal.pgen.1007424. PubMed PMID: 29852001; PubMed Central PMCID: PMCPMC6007933.
39. Hedglin M, Benkovic SJ. Regulation of Rad6/Rad18 Activity During DNA Damage Tolerance. Annu Rev Biophys. 2015;44:207-28. Epub 2015/06/23. doi: 10.1146/annurev-biophys-060414-033841. PubMed PMID: 26098514; PubMed Central PMCID: PMCPMC5592839.
40. Thon G, Klar AJ. Directionality of fission yeast mating-type interconversion is controlled by the location of the donor loci. Genetics. 1993;134(4):1045-54. PubMed PMID: 8375648; PubMed Central PMCID: PMCPMC1205573.
41. Roguev A, Schaft D, Shevchenko A, Aasland R, Shevchenko A, Stewart AF. High conservation of the Set1/Rad6 axis of histone 3 lysine 4 methylation in budding and fission

yeasts. J Biol Chem. 2003;278(10):8487-93. doi: 10.1074/jbc.M209562200. PubMed PMID: 12488447.

42. Trievel RC, Beach BM, Dirk LM, Houtz RL, Hurley JH. Structure and catalytic mechanism of a SET domain protein methyltransferase. Cell. 2002;111(1):91-103. Epub 2002/10/10. doi: 10.1016/s0092-8674(02)01000-0. PubMed PMID: 12372303.
43. Williamson K, Schneider V, Jordan RA, Mueller JE, Henderson Pozzi M, Bryk M. Catalytic and functional roles of conserved amino acids in the SET domain of the S. cerevisiae lysine methyltransferase Set1. PLoS One. 2013;8(3):e57974. Epub 2013/03/08. doi: 10.1371/journal.pone.0057974. PubMed PMID: 23469257; PubMed Central PMCID: PMCPMC3585878.
44. Krogan NJ, Dover J, Wood A, Schneider J, Heidt J, Boateng MA, et al. The Paf1 complex is required for histone h3 methylation by COMPASS and Dot1p: Linking transcriptional elongation to histone methylation. Molecular Cell. 2003;11(3):721-9. doi: Doi 10.1016/S1097-2765(03)00091-1. PubMed PMID: WOS:000182049700017.
45. Ng HH, Robert F, Young RA, Struhl K. Targeted recruitment of Set1 histone methylase by elongating Pol II provides a localized mark and memory of recent transcriptional activity. Mol Cell. 2003;11(3):709-19. Epub 2003/04/02. doi: 10.1016/s1097-2765(03)00092-3. PubMed PMID: 12667453.
46. Wood A, Schneider J, Dover J, Johnston M, Shilatifard A. The Paf1 complex is essential for histone monoubiquitination by the Rad6-Bre1 complex, which signals for histone methylation by COMPASS and Dot1p. Journal of Biological Chemistry. 2003;278(37):34739-42. doi: 10.1074/jbc.C300269200. PubMed PMID: WOS:000185164400002.
47. Kim J, Guermah M, McGinty RK, Lee JS, Tang Z, Milne TA, et al. RAD6-Mediated transcription-coupled H2B ubiquitylation directly stimulates H3K4 methylation in human cells. Cell. 2009;137(3):459-71. Epub 2009/05/05. doi: 10.1016/j.cell.2009.02.027. PubMed PMID: 19410543; PubMed Central PMCID: PMCPMC2678028.
48. Mbogning J, Nagy S, Page V, Schwer B, Shuman S, Fisher RP, et al. The PAF complex and Prf1/Rtf1 delineate distinct Cdk9-dependent pathways regulating transcription elongation in fission yeast. PLoS Genet. 2013;9(12):e1004029. Epub 2014/01/05. doi: 10.1371/journal.pgen.1004029. PubMed PMID: 24385927; PubMed Central PMCID: PMCPMC3873232.
49. Sadeghi L, Prasad P, Ekwall K, Cohen A, Svensson JP. The Paf1 complex factors Leo1 and Paf1 promote local histone turnover to modulate chromatin states in fission yeast. EMBO Rep. 2015;16(12):1673-87. doi: 10.15252/embr.201541214. PubMed PMID: 26518661; PubMed Central PMCID: PMCPMC4687421.
50. Jih G, Iglesias N, Currie MA, Bhanu NV, Paulo JA, Gygi SP, et al. Unique roles for histone H3K9me states in RNAi and heritable silencing of transcription. Nature. 2017;547(7664):463-7. doi: 10.1038/nature23267. PubMed PMID: 28682306; PubMed Central PMCID: PMCPMC5576860.
51. Wang X, Moazed D. DNA sequence-dependent epigenetic inheritance of gene silencing and histone H3K9 methylation. Science. 2017;356(6333):88-91. Epub 2017/03/18. doi: 10.1126/science.aaj2114. PubMed PMID: 28302794; PubMed Central PMCID: PMCPMC5718040.
52. Greenstein RA, Jones SK, Spivey EC, Rybarski JR, Finkelstein IJ, Al-Sady B. Noncoding RNA-nucleated heterochromatin spreading is intrinsically labile and requires accessory elements for epigenetic stability. Elife. 2018;7. Epub 2018/07/19. doi: 10.7554/eLife.32948. PubMed PMID: 30020075; PubMed Central PMCID: PMCPMC6070336.
53. Tanny JC, Erdjument-Bromage H, Tempst P, Allis CD. Ubiquitylation of histone H2B controls RNA polymerase II transcription elongation independently of histone H3

methylation. Genes Dev. 2007;21(7):835-47. doi: 10.1101/gad.1516207. PubMed PMID: 17374714; PubMed Central PMCID: PMCPMC1838534.

54. Schneider J, Wood A, Lee JS, Schuster R, Dueker J, Maguire C, et al. Molecular regulation of histone H3 trimethylation by COMPASS and the regulation of gene expression. Mol Cell. 2005;19(6):849-56. Epub 2005/09/20. doi: 10.1016/j.molcel.2005.07.024. PubMed PMID: 16168379.
55. Xhemalce B, Kouzarides T. A chromodomain switch mediated by histone H3 Lys 4 acetylation regulates heterochromatin assembly. Genes Dev. 2010;24(7):647-52. doi: 10.1101/gad.1881710. PubMed PMID: 20299449; PubMed Central PMCID: PMCPMC2849121.
56. Yu C, Bonaduce MJ, Klar AJ. Going in the right direction: mating-type switching of Schizosaccharomyces pombe is controlled by judicious expression of two different swi2 transcripts. Genetics. 2012;190(3):977-87. doi: 10.1534/genetics.111.137109. PubMed PMID: 22209903; PubMed Central PMCID: PMCPMC3296259.
57. Mahesh B. Chandrasekharan FH, and Zu-Wen Sun. Ubiquitination of histone H2B regulates chromatin dynamics by enhancing nucleosome stability. P Natl Acad Sci USA. 2009;106(39):16686-91. doi: 10.1073/pnas.0907862106. PubMed PMID: WOS:000270305800028.
58. Batta K, Zhang Z, Yen K, Goffman DB, Pugh BF. Genome-wide function of H2B ubiquitylation in promoter and genic regions. Genes Dev. 2011;25(21):2254-65. Epub 2011/11/08. doi: 10.1101/gad.177238.111. PubMed PMID: 22056671; PubMed Central PMCID: PMCPMC3219230.
59. Moyal L, Lerenthal Y, Gana-Weisz M, Mass G, So S, Wang SY, et al. Requirement of ATM-dependent monoubiquitylation of histone H2B for timely repair of DNA double-strand breaks. Mol Cell. 2011;41(5):529-42. Epub 2011/03/03. doi: 10.1016/j.molcel.2011.02.015. PubMed PMID: 21362549; PubMed Central PMCID: PMCPMC3397146.
60. Nakamura K, Kato A, Kobayashi J, Yanagihara H, Sakamoto S, Oliveira DV, et al. Regulation of Homologous Recombination by RNF20-Dependent H2B Ubiquitination. Mol Cell. 2011;41(5):515-28. Epub 2011/03/03. doi: 10.1016/j.molcel.2011.02.002. PubMed PMID: 21362548.
61. Hung SH, Wong RP, Ulrich HD, Kao CF. Monoubiquitylation of histone H2B contributes to the bypass of DNA damage during and after DNA replication. Proc Natl Acad Sci U S A. 2017;114(11):E2205-E14. Epub 2017/03/02. doi: 10.1073/pnas.1612633114. PubMed PMID: 28246327; PubMed Central PMCID: PMCPMC5358361.
62. Challa K, Schmid CD, Kitagawa S, Cheblal A, Iesmantavicius V, Seeber A, et al. Damage-induced chromatome dynamics link Ubiquitin ligase and proteasome recruitment to histone loss and efficient DNA repair. Mol Cell. 2021;81(4):811-29 e6. Epub 2021/02/03. doi: 10.1016/j.molcel.2020.12.021. PubMed PMID: 33529595.
63. Motamedi MR, Hong EJ, Li X, Gerber S, Denison C, Gygi S, et al. HP1 proteins form distinct complexes and mediate heterochromatic gene silencing by nonoverlapping mechanisms. Mol Cell. 2008;32(6):778-90. doi: 10.1016/j.molcel.2008.10.026. PubMed PMID: 19111658; PubMed Central PMCID: PMCPMC2735125.
64. Aygun O, Mehta S, Grewal SI. HDAC-mediated suppression of histone turnover promotes epigenetic stability of heterochromatin. Nat Struct Mol Biol. 2013;20(5):547-54. doi: 10.1038/nsmb.2565. PubMed PMID: 23604080; PubMed Central PMCID: PMCPMC3661211.
65. Ekwall K, Thon G. Setting up Schizosaccharomyces pombe Crosses/Matings. Cold Spring Harb Protoc. 2017;2017(7):pdb prot091694. doi: 10.1101/pdb.prot091694. PubMed PMID: 28679701.

66. Kimura H, Hayashi-Takanaka Y, Goto Y, Takizawa N, Nozaki N. The organization of histone H3 modifications as revealed by a panel of specific monoclonal antibodies. Cell Struct Funct. 2008;33(1):61-73. doi: DOI 10.1247/csf.07035. PubMed PMID: WOS:000260084000005.
67. Hayashi-Takanaka Y, Yamagata K, Wakayama T, Stasevich TJ, Kainuma T, Tsurimoto T, et al. Tracking epigenetic histone modifications in single cells using Fab-based live endogenous modification labeling. Nucleic Acids Research. 2011;39(15):6475-88. doi: 10.1093/nar/gkr343. PubMed PMID: WOS:000294555800021.

Figure Legends

Fig 1. Mating-type switching in *S. pombe*.

(A) Schematic representation of the mating-type region. The expressed *mat1* cassette containing either P (blue) or M (yellow) mating-type genes and the silenced donor cassettes, *mat2-P* and *mat3-M* are located in a heterochromatic region bordered by the *IR-L* and *IR-R* repeats. (B) Donor preference of mating-type switching. Each *mat* cassette is flanked by the homology boxes *H2* and *H1*, *mat2-P* and *mat3-M* have in addition a *H3* box. An imprinting site converted to a single-ended double-strand break (DSB) during DNA replication is located at the junction of *mat1* and its *H1* homology box (depicted here as a red star). Donor preference is determined by the information at *mat1*: *mat1-P* cells select *mat3-M* (~90%) and *mat1-M* cells select *mat2-P* (~90%). Red arrows show Atf1-Pcr1 heterodimer binding sites.

Fig 2. HULC is involved in MTS.

(A) Multiplex PCR was used to measure the content of *mat1* using primers that bind specifically to either *mat1-P* or *mat1-M* together with a *mat1*-specific primer. The P and M band intensities were measured. The graph shows the mean value ± standard deviation (SD) for four independent colonies of a WT (h^{90}) or single deletion mutants of each of the subunits of HULC and *rad18*. (B) Iodine staining of mutants lacking individual HULC subunits and a *rad18*Δ strain. WT (h^{90}) colonies capable of forming spores stain darkly by exposure to iodine vapors due to the high content of starch within the spore wall. Colonies deficient in MTS stain lightly. (C) Quantification of *mat1* content estimated by multiplex PCR. Mean values ± SD of the % of P band intensity are displayed for four independent colonies of the single *shf1*Δ mutant (same samples as in A) and for double deletion mutants combining *shf1*Δ with deletions affecting other HULC subunits. (D) Spot test using single deletion mutants of the HULC subunits and the *rad18*Δ mutant on a rich medium (YES) where a plate was subjected to UV radiation (100 J/m^2). Five-fold dilution series are shown.

Fig 3. Analysis of donor preference in HULC mutants.

(A) Quantification of *mat1* content in the h^{09} strain, of which the donor loci are swapped from *mat2-P mat3-M* to *mat2-M mat3-P*, by multiplex PCR. Mean values ± SD of the % of P band intensity of four independent colonies for single deletion mutants in each subunit of HULC in the h^{09} background. (B) Quantification of *mat1* content of mutants of *SRE* elements, *SRE3*Δ, *SRE2*Δ by multiplex PCR. Mean values ± SD of % of P band intensity of four or three independent colonies of strains with the mutated *SRE* element mutants, *SRE3*Δ and *SRE2*Δ.

Two-tailed paired Student's t test was used to compare the mean of each sample to control, n.s, not significant.

Fig 4. Analysis of histone modifications by HULC and Set1C in MTS.

(A-E) Quantification of *mat1* content by multiplex PCR. Mean value ± SD of the % of P band intensity of four or six independent colonies, showing an epistasis analysis with *set1*Δ and *shf1*Δ (A), H2B-K119R mutation in an *shf1*$^{+}$ or *shf1*Δ background (B), H3K4R mutation in a *set1*$^{+}$ or *set1*Δ background (C), *swd1*Δ, the catalytically dead Set1 (Set1-Y897A) single mutant and *swd1*Δ Set1-Y897A double mutant (D) and deletion mutants of Paf1C subunits, *leo1*Δ and *paf1*Δ (E). Two-tailed paired Student's t test was used to compare the mean of each sample, n.s, not significant.

Fig 5. Shf1 and Set1 affect the enrichments of Swi6, H3K9me2 and -me3 in the *mat* silenced region.

(A) Primer annealing sites used for qPCR: *SRE2*, K located between *SRE2* and *cenH*, and *SRE3*. (B-D) ChIP-qPCR analysis of enrichment levels relative to *act1* in P and M cells in WT, *shf1*Δ or *set1*Δ backgrounds for Swi6 (B), H3K9me2 (C) and H3K9me3 (D). Error bars indicate SD (n=3 or 4). Two-tailed paired Student's t test was used to compare the mean obtained for each gene deletion to WT of the same mating-type, *P < 0.05; **P < 0.01; ***P < 0.01; n.s, not significant.

Fig 6. Set1 works in different pathway as Dcr1 for gene silencing and MTS.

(A) Schematic view of the mating-type region of a h^{90} strain containing a *ura4* reporter gene (PG1899). Red arrows indicate binding sites for Atf1-Pcr1 dimers (B) Silencing in PG1899 was assayed by plating ten-fold dilution series of cells with the indicated gene deletions on YES medium or medium containing 5-FOA. (C) Quantification of *mat1* content by multiplex PCR, showing the % of P band intensity for the strains analyzed in the silencing assay in (B). Error bars indicate SD (n=3). (D) Proposed model for regulation of MTS involving HULC and Set1C. In M cells, HULC and Set1C inhibit the *mat3-M* donor choice at *SRE3*. Swi6 enrichments are also regulated by HULC and Set1C at *SRE2* and *SRE3*. The Swi2-Swi5 complex associates with *SRE2* and *SRE3* in a Swi6-dependent or -independent manner and promotes *mat2-P* donor choice at *SRE2* by an unknown mechanism. In P cells, the Swi2-Swi5 complex localizes at *SRE3* specifically and promotes *mat3-M* donor choice.

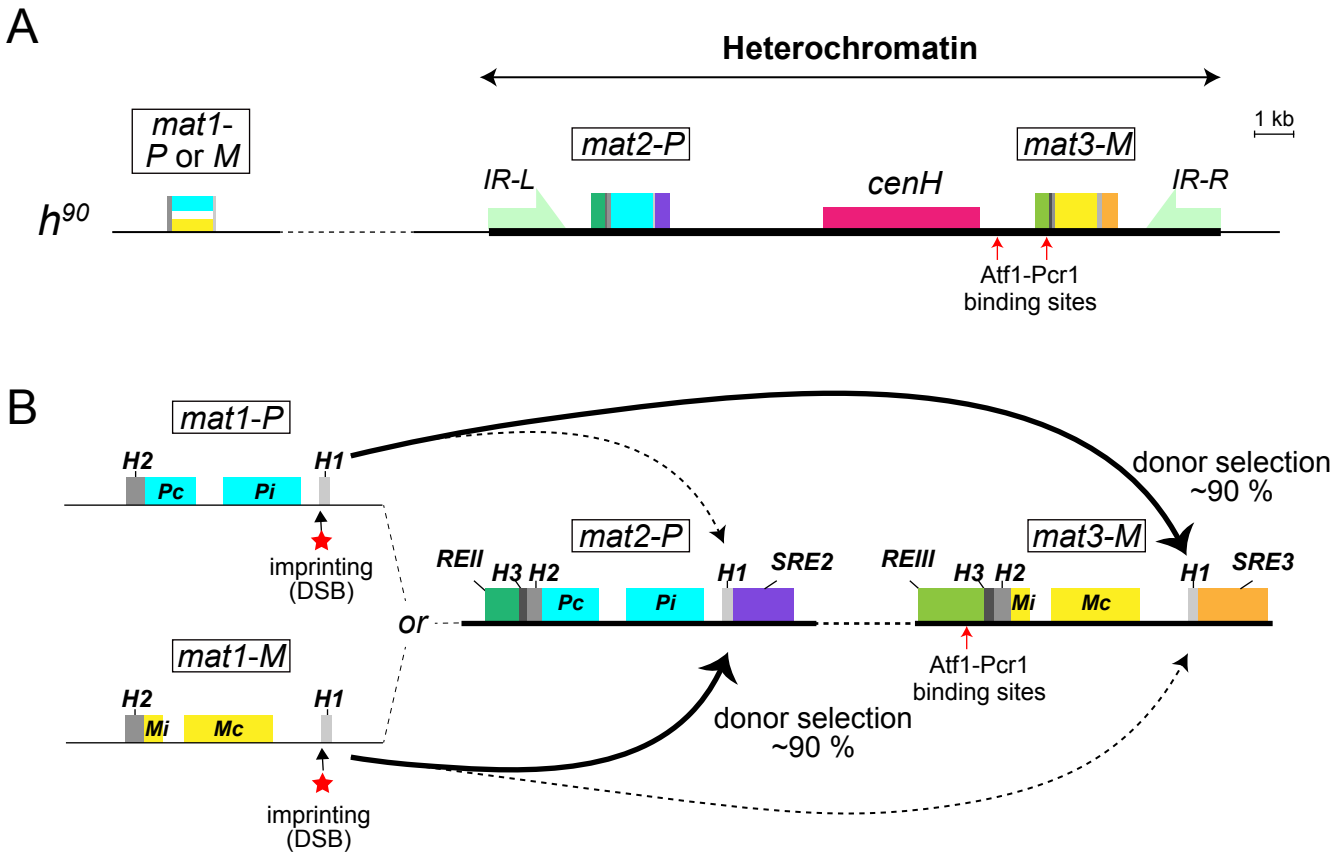

Fig 1. Chavez et al.

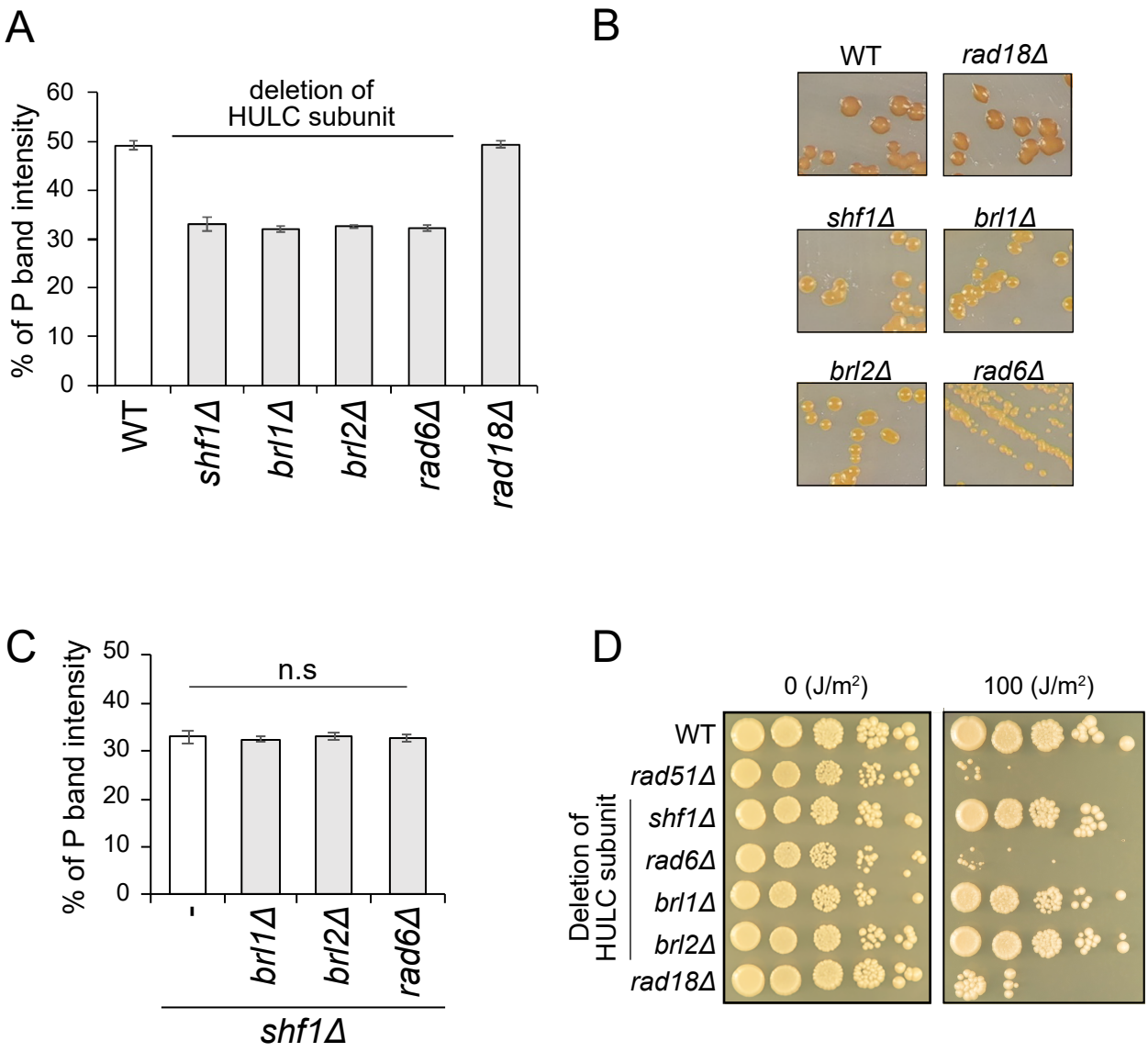

Fig 2. Chavez et al.

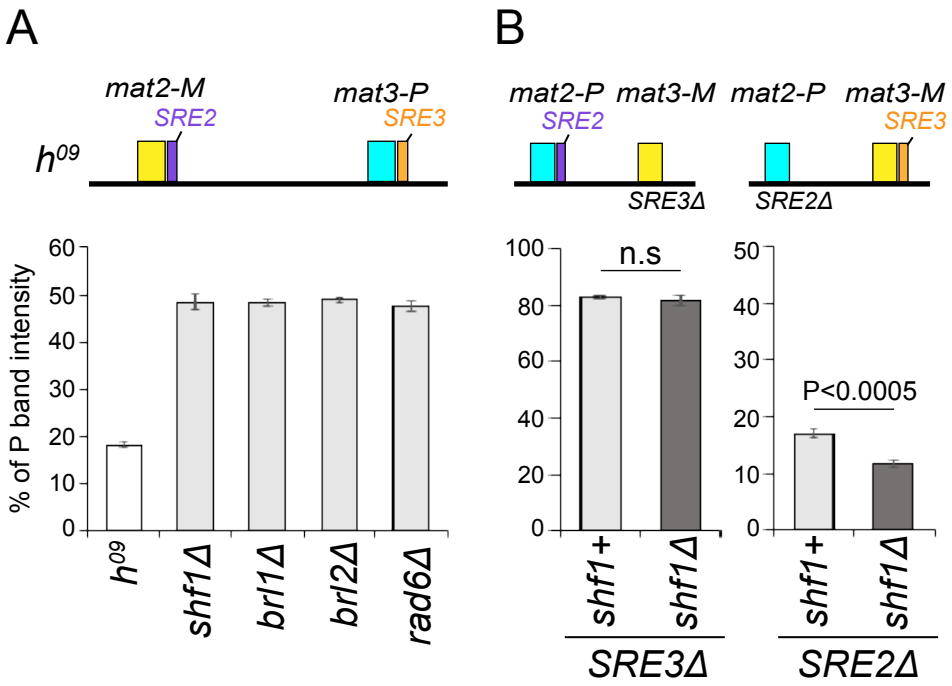

Fig 3. Chavez et al.

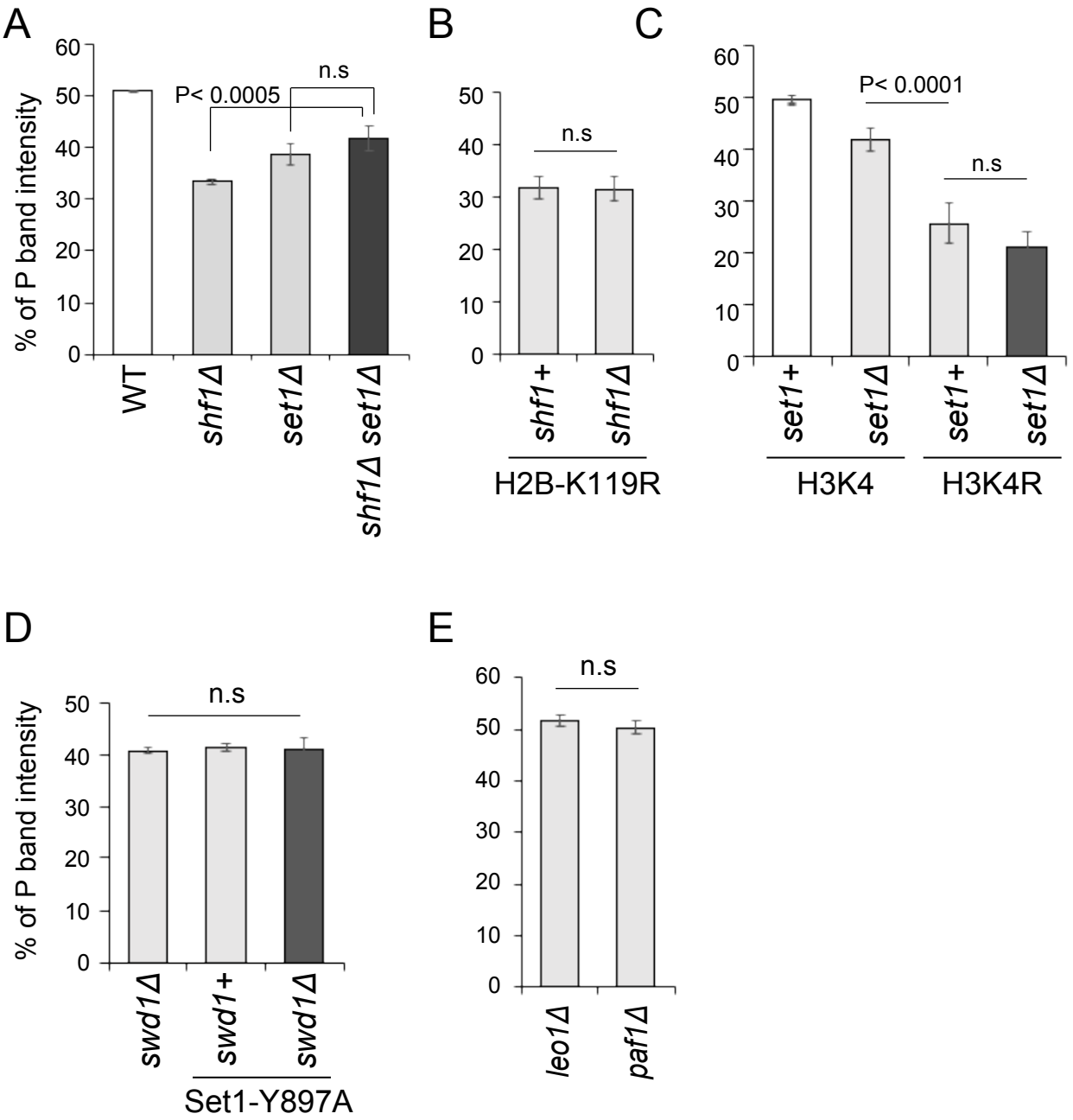

Fig. 4. Chavez et al.

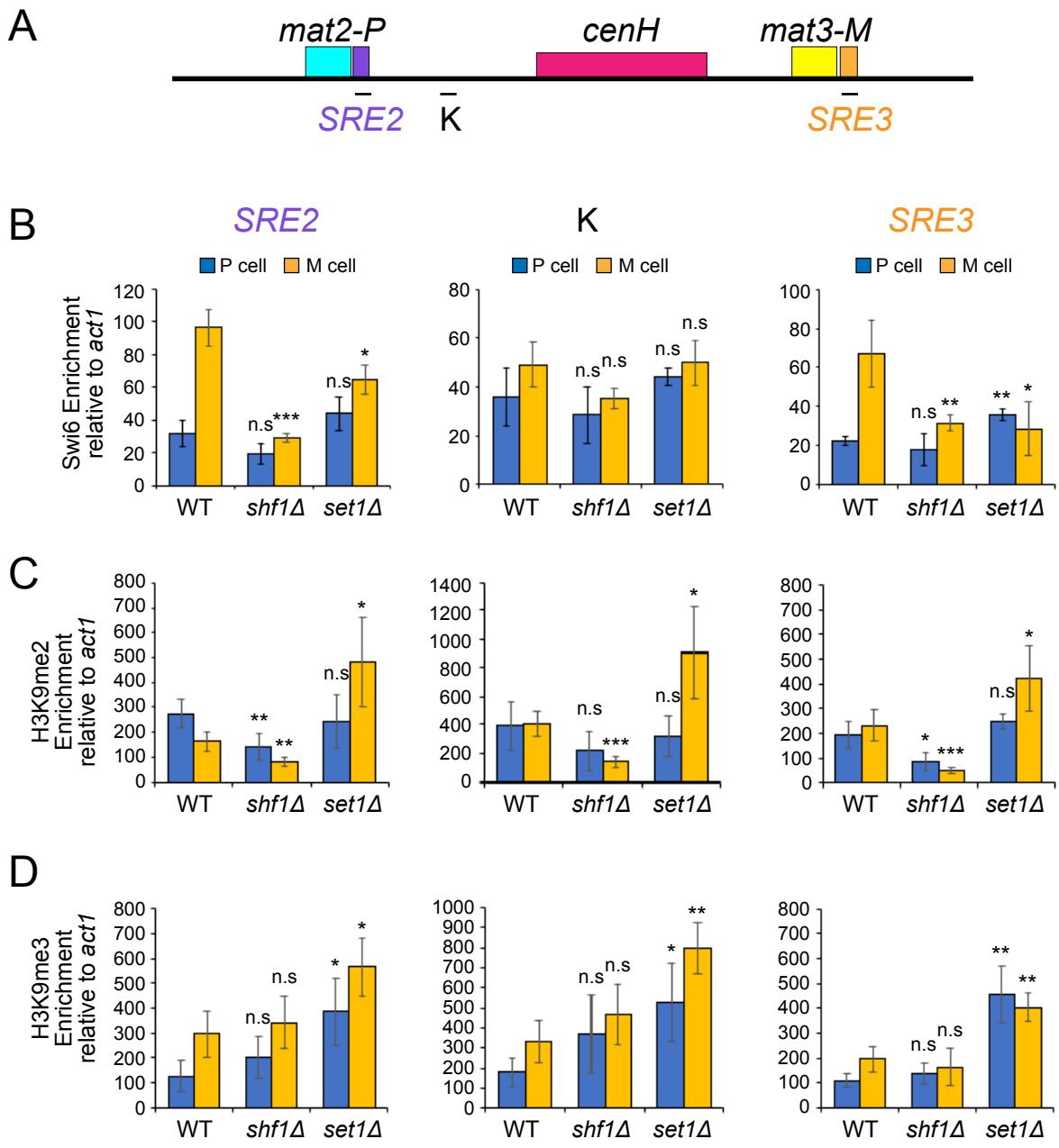

Fig. 5. Chavez et al.

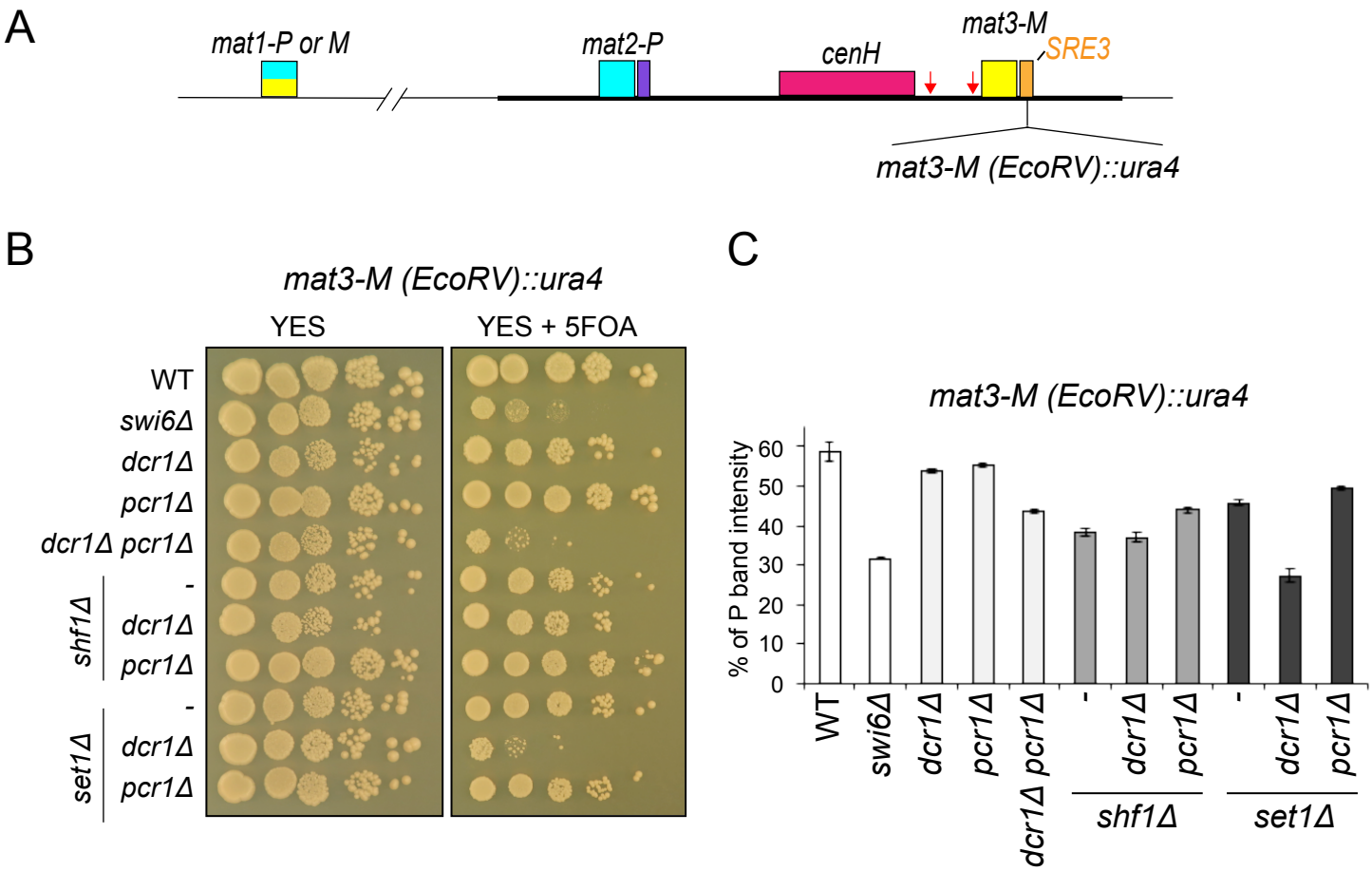

Fig 6. Chavez et al.

A

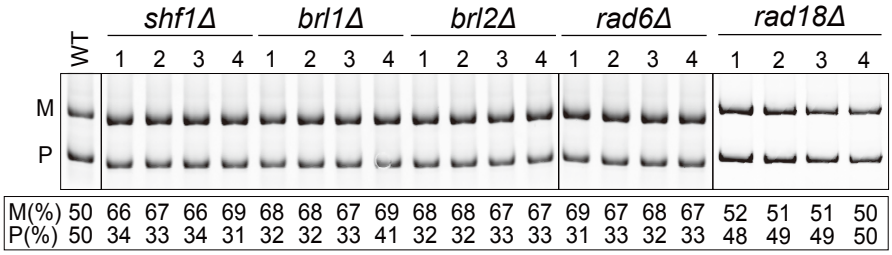

B

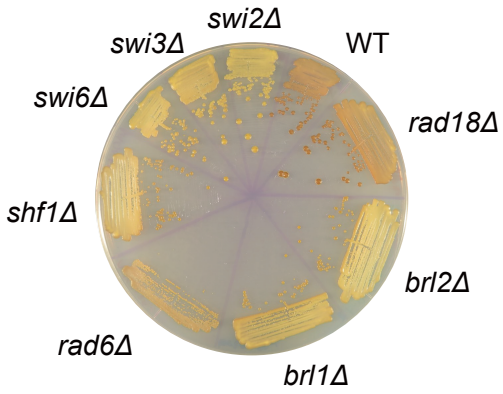

C

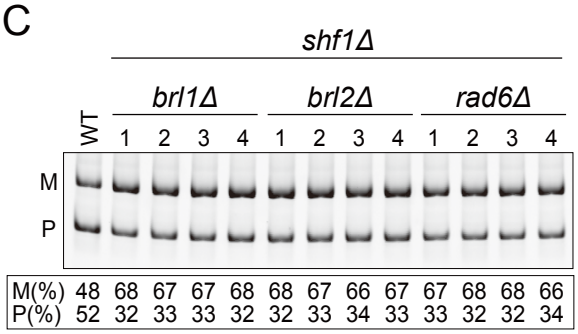

Supplementary Fig S1.Chavez et al.

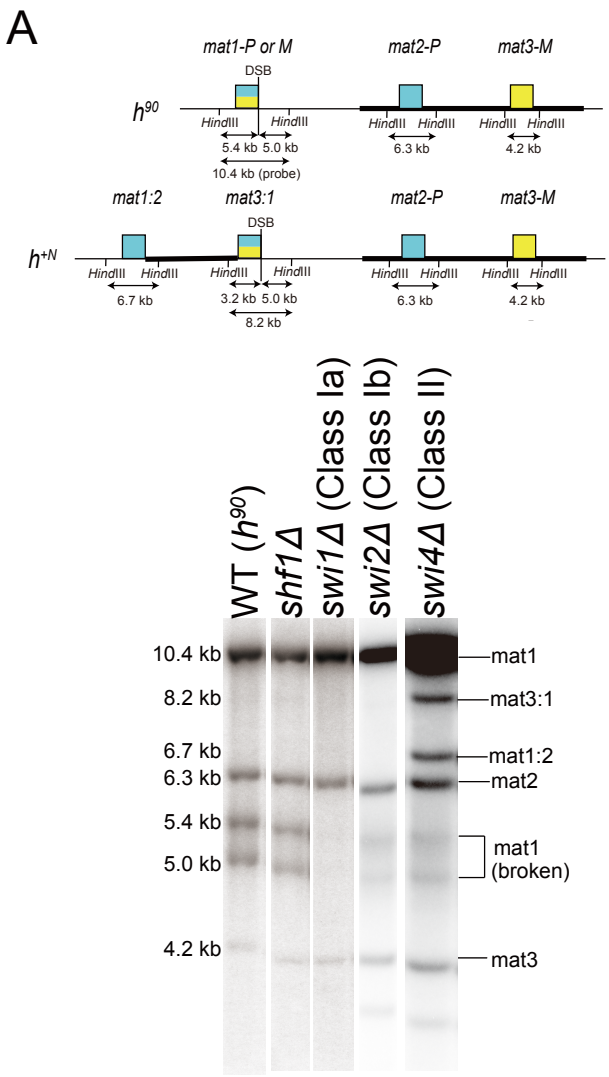

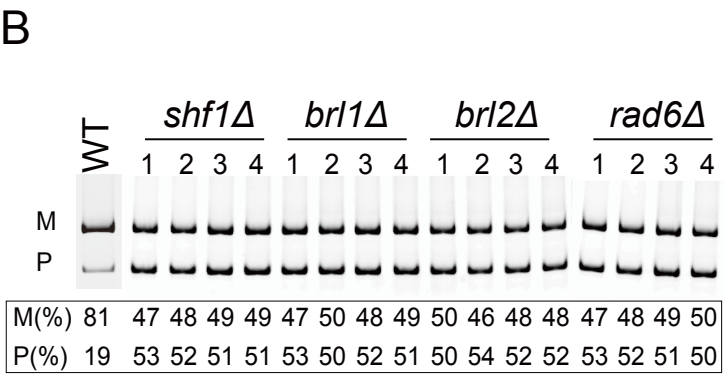

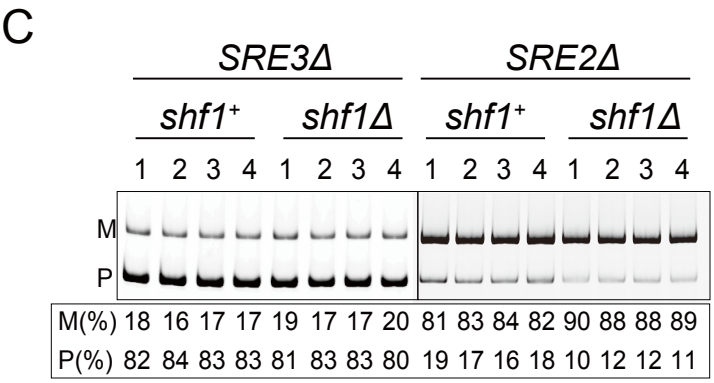

Supplementary Fig S2.Chavez et al.

A

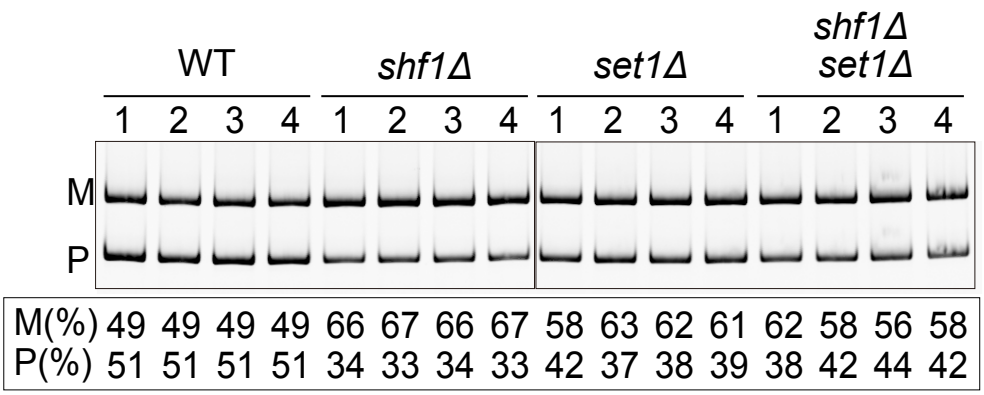

B

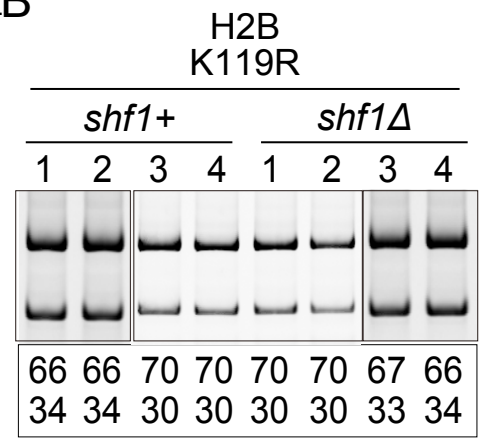

C

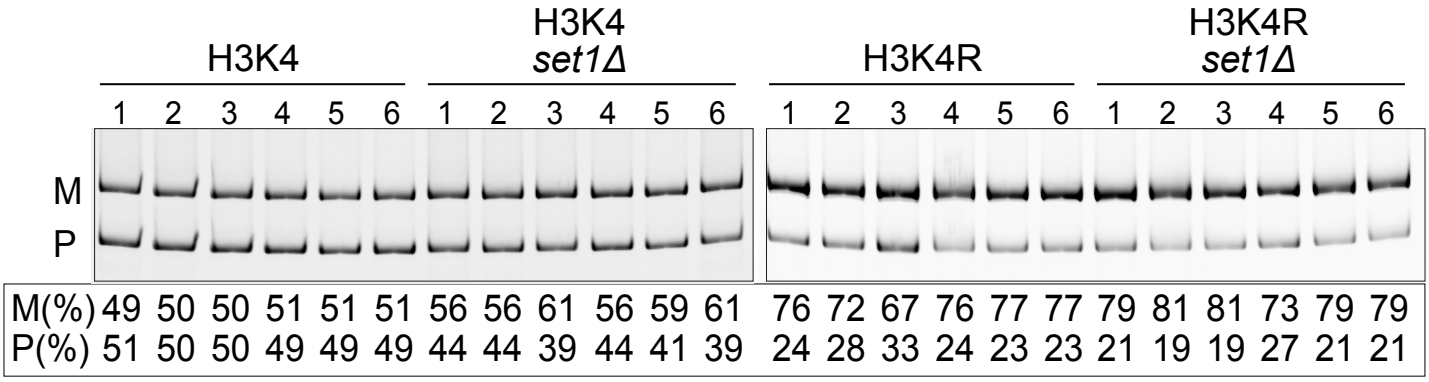

D

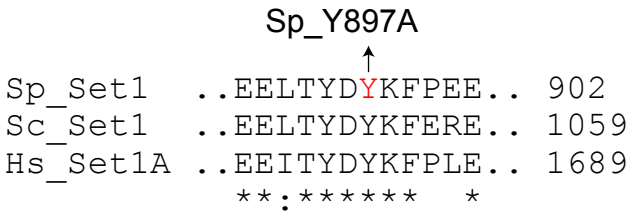

E

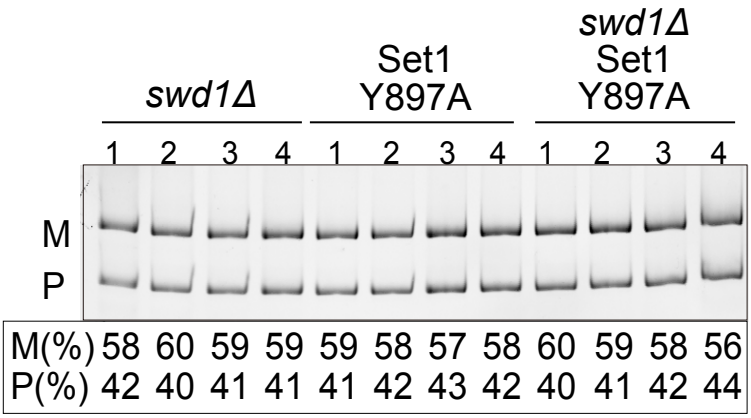

F

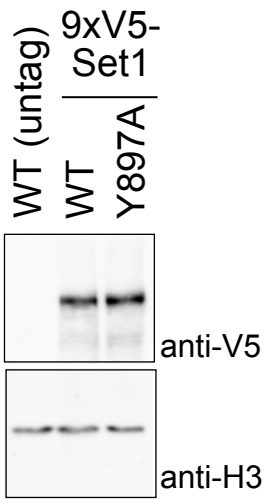

G

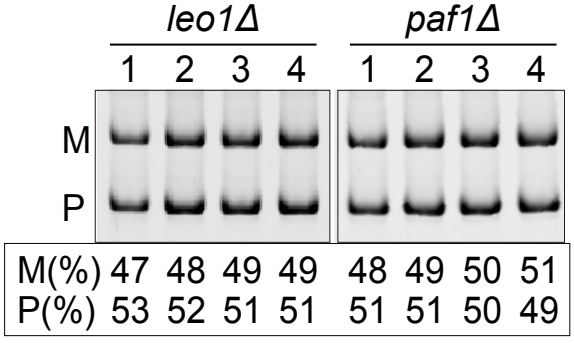

Supplementary Fig S3.Chavez et al.

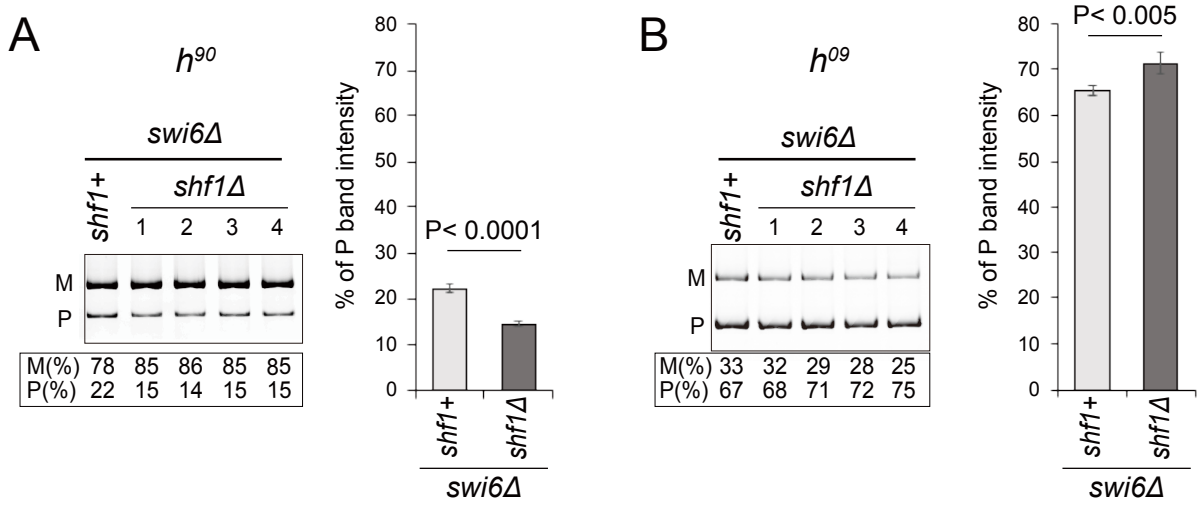

Supplementary Fig S4.Chavez et al.

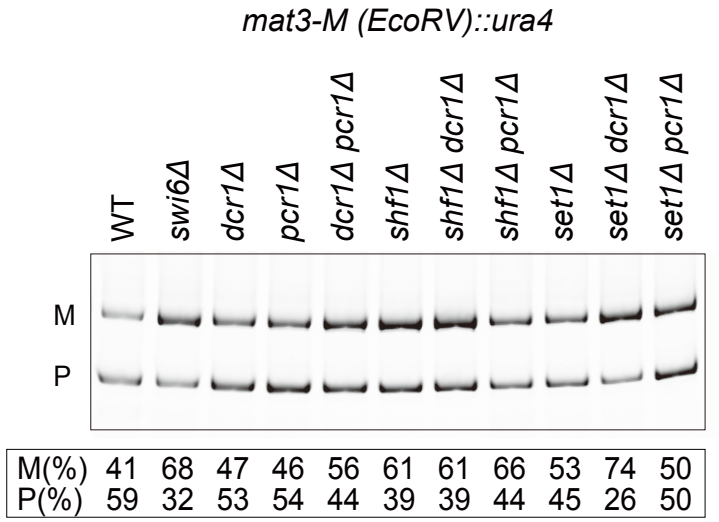

	WT	swi6Δ	dcr1Δ	pcr1Δ	dcr1Δ pcr1Δ	shf1Δ	shf1Δ dcr1Δ	shf1Δ pcr1Δ	set1Δ	set1Δ dcr1Δ	set1Δ pcr1Δ
M(%)	41	68	47	46	56	61	61	66	53	74	50
P(%)	59	32	53	54	44	39	39	44	45	26	50

Supplementary Fig S5.Chavez et al.